

Electronic Supplementary Information

A Porous Ru Nanomaterial as Efficient Electrocatalyst for the Hydrogen Evolution Reaction in Acidic and Neutral Conditions

S. Drouet,^{*a,b} J. Creus,^{a,b,c} V. Collière,^{a,b} C. Amiens,^{a,b} J. García-Antón,^c X. Sala^c and K. Philippot^{*a,b}

¹ Laboratoire de Chimie de Coordination du CNRS, 205 route de Narbonne, F-31077, Toulouse Cedex 04 (France)

² Université de Toulouse, UPS, INPT, LCC, F-31077 Toulouse Cedex 04 (France)

³ Departament de Química, Facultat de Ciències, Universitat Autònoma de Barcelona, 08193 Bellaterra, Catalonia (Spain).

Experimental Section

Materials. All operations for the synthesis of the Ru/THF/MeOH nanomaterial were carried out using standard Schlenk tubes, Fisher–Porter bottle techniques or in a glove-box (MBraun) under argon atmosphere. Solvents (THF and MeOH) were purified before use, by filtration on adequate column in a purification apparatus (MBraun) for THF and by distillation on magnesium for MeOH, and handled under argon atmosphere. Solvents were degassed before use according to a freeze–pump–thaw process. The ruthenium precursor, [Ru(cod)(cot)] was purchased from Nanomeps-Toulouse. Hydrogen gas (Alphagaz) was purchased from Air Liquide. High purity deionized water was obtained by passing distilled water through a nanopore Milli-Q water purification system.

Synthesis of Ru NPs. 100 mg of [Ru(cod)(cot)] were dissolved under argon in a total volume of 100 mL of a MeOH/THF mixture (5:95) in a Fisher porter reactor inside a Glove-box. After pressurization of the reactor with 3 bar of H₂ at room temperature (r.t.), the initial yellow solution turned dark brown in a few minutes. A vigorous magnetic stirring and the H₂ pressure were maintained for 45 minutes. After this reaction time, the H₂ pressure was evacuated and a drop of the colloidal solution was deposited onto a carbon-covered copper grid for microscopy analysis. The Ru nanomaterial was isolated as a grey powder after simple evaporation to dryness under vacuum.

Characterization. The colloidal solution has been characterized by Transmission Electron microscopy (TEM), High resolution electron microscopy (HREM) and the isolated solid by powder X-ray diffraction (XRD) and X-Ray photoelectron spectroscopy (XPS).

Powder X-Ray Diffraction measurements were performed with a PANalytical X'Pert Pro θ/θ diffractometer equipped with a X'Celerator detector using Cu radiation ($\lambda = 1.5418 \text{ \AA}$). The data were registered in the 2θ range $2-90^\circ$ with a step wise of 0.016° and a time by step equal to 1000s. Highscore software was used for data analysis.

Transmission Electron Microscopy (TEM) and High resolution TEM (HR-TEM). Samples for transmission electron microscopy (TEM) and high-resolution HR-TEM analyses were prepared by slow evaporation of a drop of the crude colloidal solution deposited onto a holey carbon-covered copper grid. TEM and HR-TEM analyses were performed on a MET JEOL JEM 1011 microscope operating at 100 kV with a resolution point of 0.45 nm and a JEOL JEM-ARM 200F microscope working at 200 kV with a resolution point lower of 0.19 nm, respectively. TEM allowed to evaluate the particle size, size distribution and morphology. Enlarged micrographs were used for treatment with ImageJ software to obtain a statistical size distribution and the nanoparticle mean diameter. FFT treatments of HREM images were carried out with Digital Micrograph Version 1.80.70 to determine the crystalline structure of the material.

X-Ray Photoelectron Spectra XPS measurements were performed with a Phoibos 150 analyzer (SPECS GmbH, Berlin, Germany) in ultra-high vacuum conditions (base pressure $5E^{-10}$ mbar) with a monochromatic aluminium K α x-ray source (1486.74 eV). The energy resolution was measured by the FWHM of the Ag 3d^{5/2} peak for a sputtered silver foil was 0.62 eV.

Electrochemical measurements were performed using an Autolab (PGSTAT 302N) as potentiostat in a three-electrode configuration electrochemical cell. GC disk electrode coated with the catalyst material was used as working electrode (3 mm), Pt wire and Hg/HgSO₄ (K₂SO₄ sat) were used as a counter electrode (CE) and a reference electrode (RE), respectively. GC disk electrode was carefully polished and ultrasonically rinsed for 10 min, both in ethanol and water. Both the CE and RE were rinsed with distilled water and dried with compressed air prior measurements.

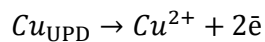
Electrode Preparation: The modified GC electrode was prepared as follows: 2.5 mg of electrocatalyst was added into 100 μL of n-propanol, 2 μL of 5% Nafion and 398 μL of distilled water (Milli-Q). The mixture was ultra-sonicated for 10 min to obtain an ink. Then 5 μL of the ink were loaded onto the GC disk electrode ($S = 0.071 \text{ cm}^2$) with a micropipette. The working electrode was then dried for 1h at r.t. All potentials were converted to NHE by adding a value of 0.645 V (reference value at 25°C). The

current density was normalized over the geometric surface area of the electrode. The electrochemical studies for HER were conducted in 0.5 M H₂SO₄ (pH 0.3) solution and in 0.1 M phosphate buffer solution (pH 7) under argon, at 25°C and under continuous stirring.

Electrochemical active surface area (ECSA) determination: Double layer capacitance was estimated to determine the electrochemically active surface area (ECSA) of the catalyst. A potential range in which there is minimal faradaic current response was selected by CV. All measured current in this region is assumed to be a charging current due to double layer charging. CV measurements were performed in non-stirred solution by sweeping the potential across this non-faradaic region from the more positive to negative potential and back at different scan rates, namely: 5, 10, 25, 75, 50, 100 and 500 mV s⁻¹. The potential of the working electrode was held 10 seconds at each potential vertex before beginning the next sweep.

Under potential Deposition (UPD) of Copper. The UPD method was performed to determine the number of active sites. In an electrochemical cell, a controlled potential electrolysis was performed at 0.145 V vs. NHE for 100s in 0.5M H₂SO₄ solution with 5 mM of CuSO₄. LSV were performed before and after the CPE experiment in a free-copper solution ($E_i = 0.04$ V, $E_f = 0.89$ V, 10 mV/s). After CPE, LSV exhibit a new wave devoted to the oxidation of deposited Cu at $E = 0.41$ V vs. NHE.

The number of active sites (n) was calculated based on the UPD copper stripping charge (Q_{Cu} , Cu_{UPD}):



$$n = \frac{Q_{Cu}}{2F}$$

, where F is the Faraday constant (96485 C/mol).

TOF (s⁻¹) calculations

TOF where calculated as follows:

$$TOF(s^{-1}) = \frac{I}{2Fn} = \frac{I}{Q_{Cu}}$$

, where I is the current intensity on the LSV measurement, F is the Faradaic constant, and n the number of active sites obtained by the UPD method. The factor 1/2 is based on the consideration that two electrons are required to form one hydrogen molecule.

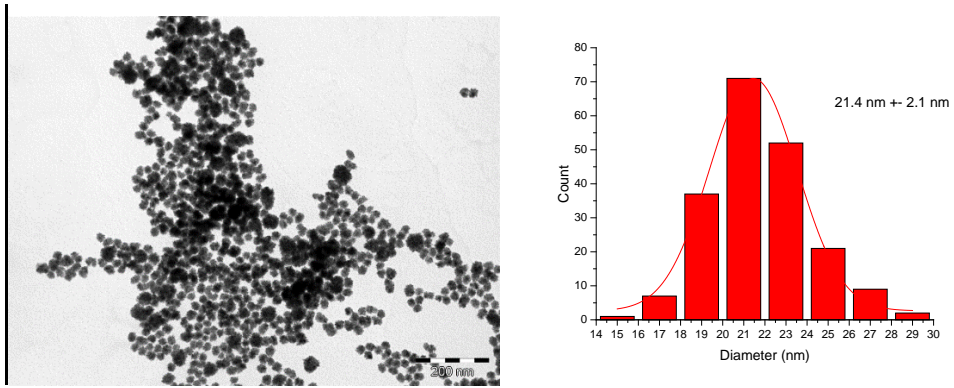


Fig. S1 TEM image and size distribution of Ru/MeOH/THF nanomaterial.

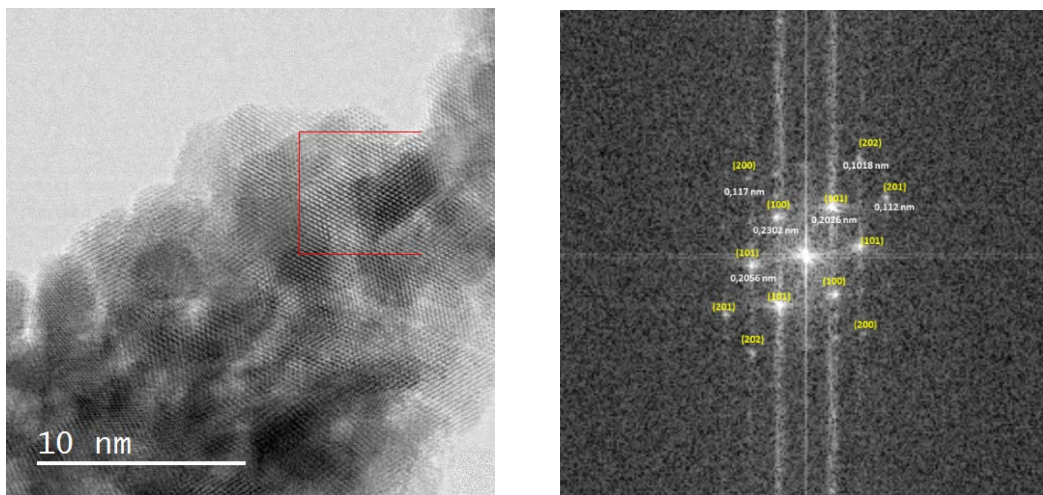


Fig. S2 HR-TEM image and corresponding FFT pattern of the Ru/MeOH/THF nanomaterial showing hcp structure

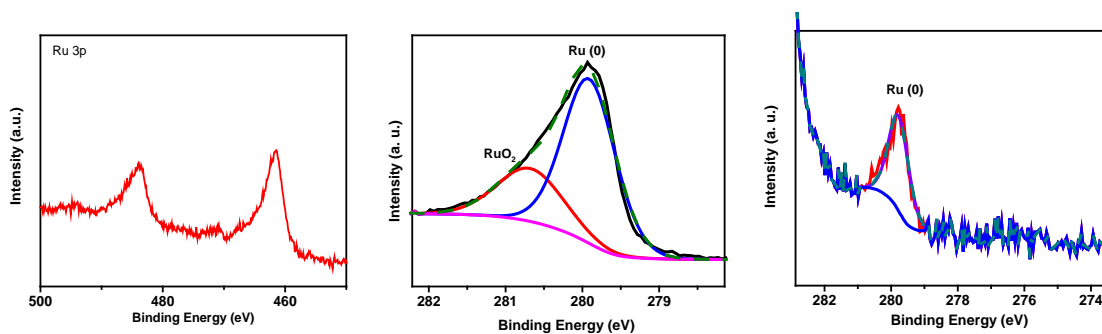


Fig. S3 XPS spectrum of Ru/MeOH/THF nanomaterial deposited on GC electrode before catalytic process (Left and middle) after CPE at -0.05 V vs NHE for 30 min in 0.5 M H₂SO₄ (Right).

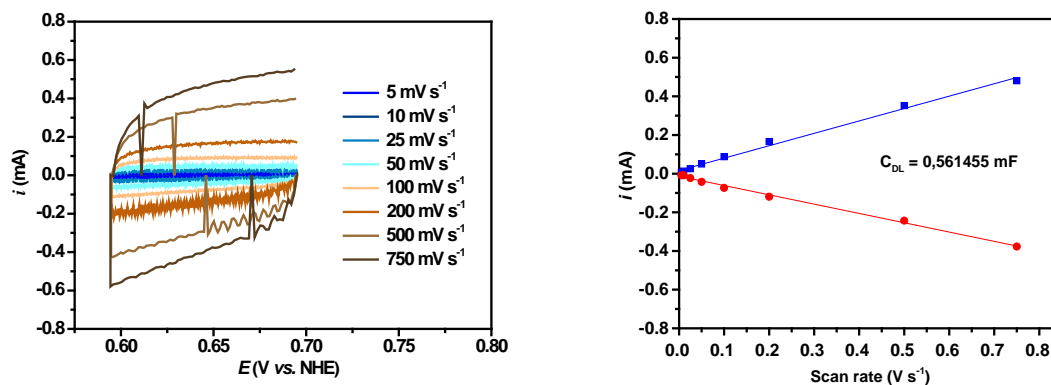


Fig. S4 (left) CV measured in a non-faradaic region at various scan rate from 750 mV s⁻¹ to 5 mV s⁻¹ in 0.5 M H₂SO₄ (right) Plot of the cathodic (red open circle) and anodic (blue open square) charging currents measured at 0.65 V vs NHE as a function of scan rate.

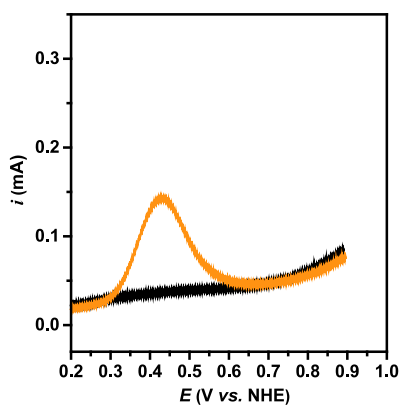


Fig. S5 LSV of Copper UPD in 0.5 M H₂SO₄ at 10 mV/s before (black) and after CPE at 0.145 V for 100 s in presence of 5 mM Cu₂SO₄. (yellow)

electrocatalyst	$\eta_{10 \text{ mA cm}^{-2}, t=0}$	$\eta_{10 \text{ mA cm}^{-2}, t=2 \text{ h}}$	Ref
Co	230	260	1
CoMo	100	100	2
Fe	740	850	3
Ni	370	470	1
NiMo	45	39	4
NiFe	220	260	3
NiW	60	110	5
Mo/S	220	250	6
NiMoCo	50	50	7
NiMoFe	90	100	8
Pt	50	60	9
Ru/MeOH/THF	99	103	This work

Table S1 Electrocatalysts benchmarking comparison following Jaramillo methodology

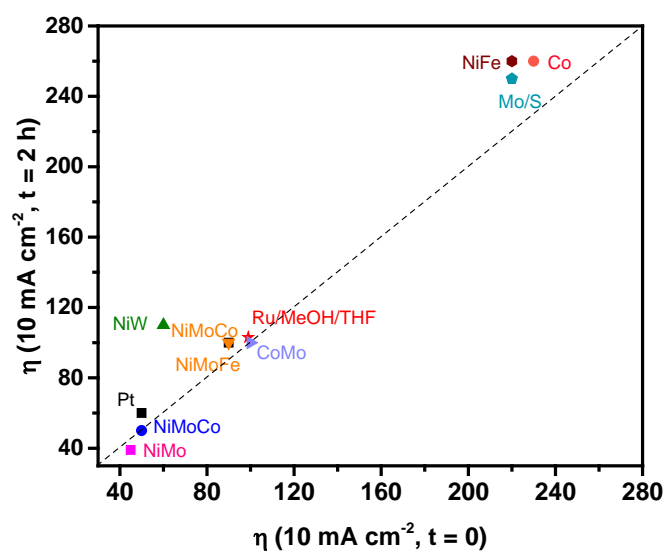


Fig. S6 Graphical representation of electrocatalysts benchmarking comparison

Electrocatalyst	Tafel slope (mV dec ⁻¹)	$\eta_{10 \mu\text{A cm}^{-2}}$ (mV)
Ru/MeOH/THF	46	83
Ru powder	60	94
Pt/C	30	58

Table S2 Electrocatalytic parameters of Ru/MeOH/THF, Ru powder and Pt/C in 0.5 M H₂SO₄.

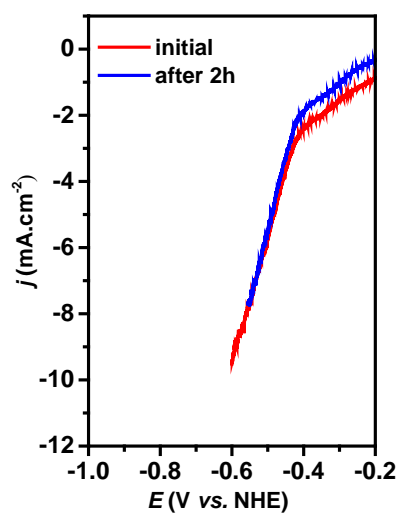


Fig. S7 LSV curves of Ru/MeOH/THF nanomaterial initial (red) and after 2h of galvanostatic experiment (blue) in 0.1 M phosphate buffer at 10 mV/s.

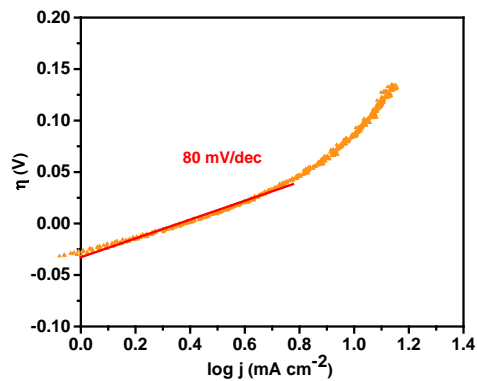


Fig. S8 Tafel plots of Ru/MeOH/THF nanomaterial in 0.1 M phosphate buffer solution.

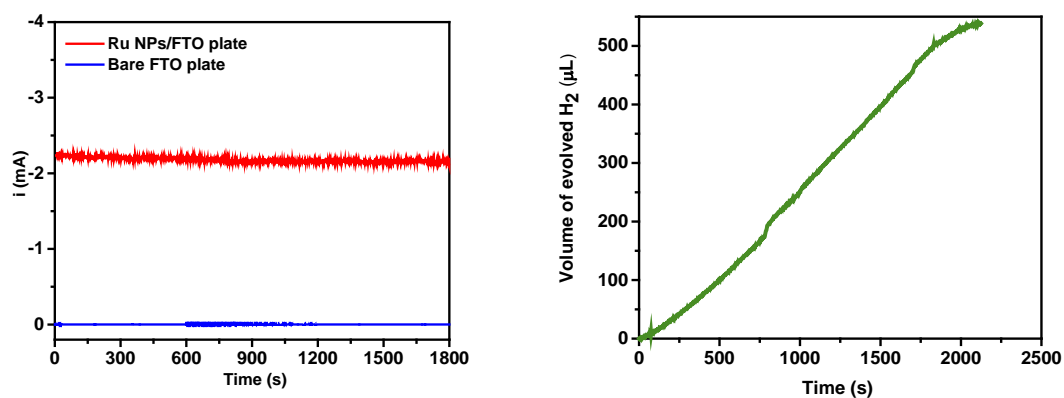


Fig. S9 (left) Controlled-potential electrolysis of Ru/MeOH/THF nanomaterial onto ITO plate in 0.5 M H_2SO_4 at -0.05 V vs. NHE (blue) CPE of bare ITO plate (red) (right) H_2 evolution profile measured by Clark electrode during CPE.

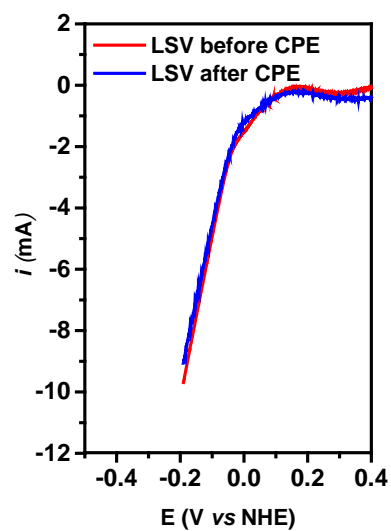


Fig. S10 LSV curves Ru/MeOH/THF nanomaterial deposited on ITO electrode before CPE (red) and after (blue) in 0.5 M H₂SO₄ solution at 10 mV/s.



Fig. S11 Picture of the CPE cell and the Ru/MeOH/THF nanomaterial deposited onto ITO electrode.

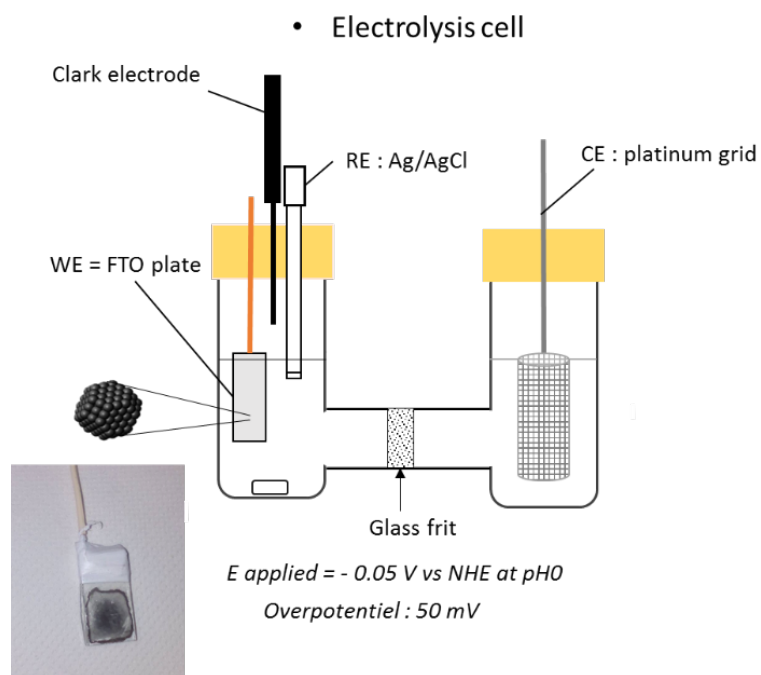


Fig. S12 Representative scheme of the electrolysis cell.

1. O. Savadogo and H. Lavoie, *Int. J. Hydrogen Energy*, 1992, **17**, 473-477.
2. C. Fan, D. L. Piron, A. Sleb and P. Paradis, *J. Electrochem. Soci.*, 1994, **141**, 382-387.
3. R. Solmaz and G. Kardaş, *Electrochim. Acta*, 2009, **54**, 3726-3734.
4. E. Navarro-Flores, Z. Chong and S. Omanovic, *J. Mol. Catal. A: Chem.*, 2005, **226**, 179-197.
5. I. A. Raj and K. I. Vasu, *J. Appl. Electrochem.*, 1990, **20**, 32-38.
6. D. Merki, H. Vrubel, L. Rovelli, S. Fierro and X. Hu, *Chem. Sci.*, 2012, **3**, 2515-2525.
7. C. Fan, D. L. Piron and P. Paradis, *Electrochim. Acta*, 1994, **39**, 2715-2722.
8. I. A. Raj and K. I. Vasu, *J. Appl. Electrochem.*, 1992, **22**, 471-477.
9. D. J. Walton, L. D. Burke and M. M. Murphy, *Electrochim. Acta*, 1996, **41**, 2747-2751.